Notes On Implementation Of Trapezoidal Shadow Maps

Eugene K. Ressler

July 26, 2011

Abstract

The Trapezoidal Shadow Map algorithm by Tobias Martin and Tiow-Seng Tan is elegant. It deserves equally elegant implementation details. Here are a few ideas in this regard.

1 Introduction

We are concerned here with implementation details of trapeziodal shadow maps as described in [1], hereinafter called "the paper." The authors, Tobias Martin and Tiow-Seng Tan, have published some useful ideas of their own [3] including partial source code [2]. In implementing the algorithm ourselves, we employed some simplifications. These are mainly of esthetic interest, which are nonetheless important. The TSM algorithm is beautiful and deserves the most beautiful implementation possible.

2 Computing the Trapezoid

The authors' code makes free use of line intersection and inverse trigonometric function calculations. We avoid these heavyweight operations through judicious use of vector products. Our most expensive arithmetic consists of square roots, and no more than seven of these to find each trapezoid.

We assume that the view frustum is already transformed to the post-perspective space of the light (PPSL) as discussed in the paper. A clear understanding of PPSL will help the reader envision the TSM algorithm without confusion. PPSL is a two-dimensional space where the scene could hypothetically be projected to depict what a virtual observer at the light source would see when looking in the light's direction. If the light is a point source, perspective division has already been applied. Otherwise it is a parallel source like the sun, and the projection is orthogonal. In this case, PPSL is a slight misnomer because no perspective is involved. The projection boundaries of the PPSL coordinate system are unimportant because they will be subsumed in the trapezoidal projection we are about to

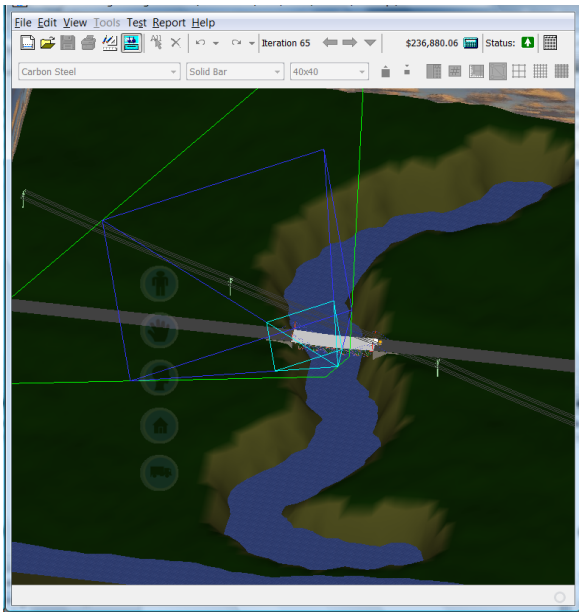

Figure 1: Frusta and trapezoid in PPSL.

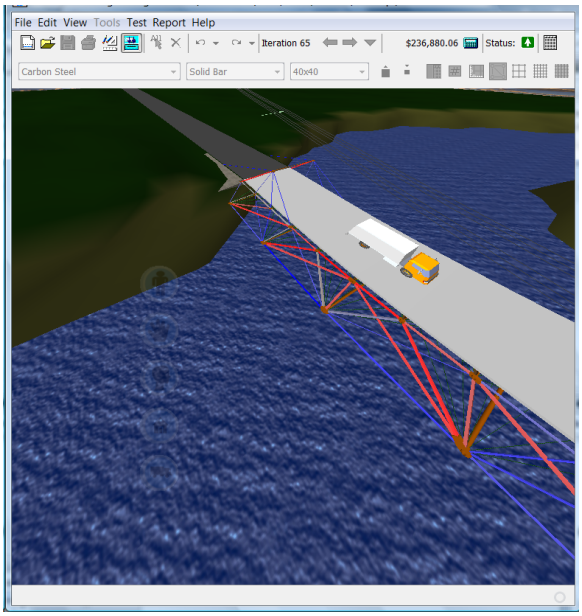

Figure 2: Scene after trapezoidal projection.

compute. This is why we say "hypothetical" above. PPSL is just a stepping stone to obtain the final trapezoidal projection. Only the view frustum world coordinates are transformed to PPSL, not the scene itself.

Figure 1 shows PPSL in our application, which has a parallel light source. The clipping boundaries of the projection have been picked for convenient viewing. Frusta for the viewing and focus regions are shown in shades of blue. They are wrapped in the trapezoid, depicted in green. Figure 2 shows the same scene after the trapezoidal projection is applied. Objects toward the viewer are enlarged.

Though we assume the PPSL convex hull of the view frustum has been calculated, this is not strictly necessary. Our method ought to work as well if the eight points of the frustum are processed in place of four to six convex hull points. The only convex hull that is strictly necessary is of the focus region so that its area can be computed when iterating to find the best value of η as described in the paper.

Figure 3 depicts the view frustum in gray, already flattened into PPSL coordinates. Points N and F are, respectively, the flattened centroids of the near and far planes. Then the *unit line-of-sight vector* is

$$\mathbf{a} = \frac{F - N}{|F - N|} \cdot \tag{1}$$

This is a very useful quantity, requiring one square root.

Let points P_i, $i = 1 \ldots n$ be the vertices of the convex hull of the frustum in PPSL. We now compute the dot products

$$t_i = (P_i - N) \cdot \mathbf{a}, \quad i = 1 \ldots n \, . \tag{2}$$

Since these values are signed distances in PPSL measured along vector $\mathbf{a}$ from point N, we

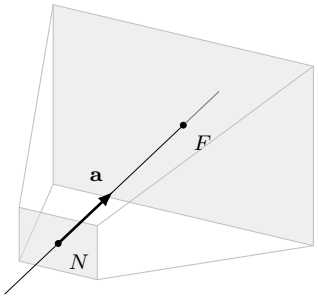

Figure 3: Axis through flattened frustum.

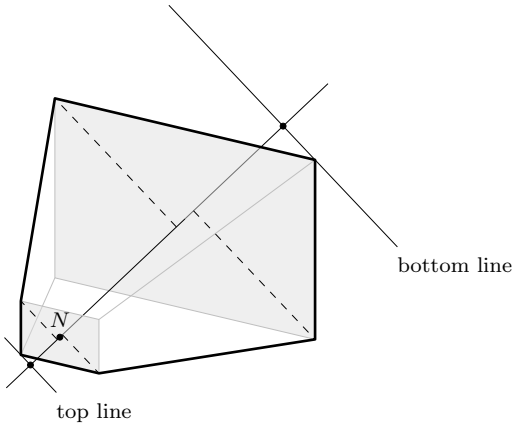

Figure 4: Hull vertices projected.

can say

$$t_T = \min_i t_i \quad \text{and} \quad t_B = \max_i t_i \tag{3}$$

are, respectively, the distances from N to the intersections of the trapezoid top and base lines with the line-of-sight. Figure 4 shows these two intersections along with projections of all other convex hull points onto the axis and the resulting top and bottom lines. In all but degenerate cases, we will have $t_T < 0$ and $t_B > 0$. Two useful facts now arise:

- It is never necessary to compute the above intersections. (The authors do.)
- Values t_T and t_B are easily computed with one pass over the convex hull. (The authors use two.)

Again because t_B and t_T are distances, λ in the paper is merely

$$\lambda = t_B - t_T \; . \tag{4}$$

The next step is to find δ', the focus distance measured in PPSL. The author's code uses a different scheme for computing this than the one implied by the diagram in the paper, which is merely to use the distance from the top line to the center of the far plane of the focus area's truncated frustum,

$$\delta' = t_F - t_T \; . \tag{5}$$

The authors used the convex hull of the truncated frustum and the distance to its farthest point from the top line. The simpler approach worked well for us.

We turn now to computing the left and right edges. Use λ and δ' to determine η with the simple 80% formula in the paper. Point Q is then given by

$$Q = N + (t_T - \eta)\mathbf{a} \; . \tag{6}$$

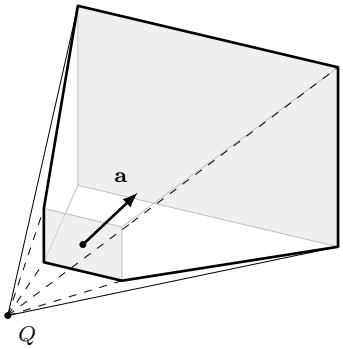

Figure 5: Left and right edge directions.

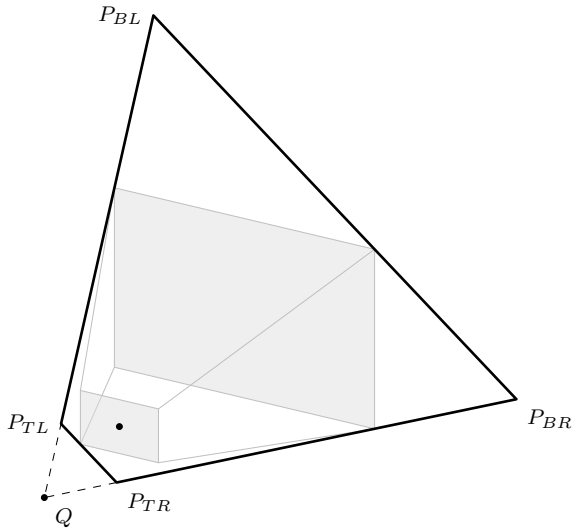

Figure 6: Complete trapezoid.

The edge directions are obtained by considering the rays connecting Q to hull vertices as shown in Figure 5. Their directions are $P_i - Q$. We want the leftmost (farthest counterclockwise) and rightmost (farthest clockwise) with respect to $\mathbf{a}$. For this, note that if $\mathbf{u}$ and $\mathbf{v}$ are arbitrary unit vectors with included angle θ, then

$$\sin\theta = x_u y_v - x_v y_u = \mathbf{u}^\perp \cdot \mathbf{v} \ , \tag{7}$$

where $\mathbf{u}^\perp = [-y_u, x_u]$ is $\mathbf{u}$ rotated by $\pi/2$ radians—the left-perpendicular of $\mathbf{u}$. Hence, we compute

$$\mathbf{u}_i = \frac{P_i - Q}{|P_i - Q|} \quad \text{and} \tag{8}$$

$$s_i = \mathbf{a}^\perp \cdot \mathbf{u}_i \ . \tag{9}$$

The values s_i are enough to find the desired leftmost and rightmost rays. The indices are simply

$$L = \arg\max_i s_i \quad \text{and} \quad R = \arg\min_i s_i \ . \tag{10}$$

No inverse trig functions are needed, only one square root per convex hull vertex—no more than six.

Let $\mathbf{u}_L$ and $\mathbf{u}_R$ be the corresponding leftmost and rightmost unit vectors, computed previously as $\mathbf{u}_i$ in Equation 8. These are enough to find the four corners of the trapezoid. In Figure 7, t may be either $t_T = \eta$, the distance from Q to the top line of the trapezoid or $t_B = \eta + \lambda$, the distance to the base. Vector $\mathbf{u}$ is either $\mathbf{u}_L$ or $\mathbf{u}_R$. Scalar x is the only

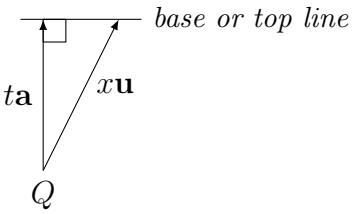

Figure 7: Solving for trapezoid corners.

unknown. Due to the right angle, we have

$$(x\mathbf{u} - t\mathbf{a}) \cdot (t\mathbf{a}) = 0 \tag{11}$$

$$xt(\mathbf{u} \cdot \mathbf{a}) = t^2(\mathbf{a} \cdot \mathbf{a}) \tag{12}$$

$$x = t/(\mathbf{u} \cdot \mathbf{a}) \; . \tag{13}$$

This implies that the trapezoid corners P_{TL}, P_{TR}, P_{BR}, and P_{BL} are given by

$$P_{ij} = Q + \frac{t_i}{\mathbf{u}_j \cdot \mathbf{a}} \mathbf{u}_j, \tag{14}$$

where $i \in \{T, B\}$ and $j \in \{L, R\}$, replacing the author's four line intersection computations. The result is shown in Figure 6.

The authors use the trapezoidal transformation as the x and y components of the OpenGL projection matrix, setting the z row to unity. It is important to remember that front and back clipping will remove all scene elements outside $[-1..1]$ when writing the depth buffer. Either the scene must be appropriately translated and scaled in z by the model-view matrix, a tricky undertaking if the scene is lit, or the z-row of the trapezoidal projection must be modified to do the job. If this scene lies within extent $[z_{\min}..z_{\max}]$ measured from the light (the pseudo eye point used to transform to PPSL), then the z row should be

$$\begin{bmatrix} 0 & 0 & \frac{2}{z_{\min} - z_{\max}} & \frac{z_{\min} + z_{\max}}{z_{\min} - z_{\max}} \end{bmatrix} \; . \tag{15}$$

A final detail is that the computed trapezoid (and rectangle as discussed below) must be given in a consistent direction—counterclockwise for default OpenGL processing. A reverse order will ultimately cause surface normals to also be reversed, which affects e.g. culling. We set out to cull front faces for shadow map rendering. An early bug was immediately evident as Moiré patterns because back faces were culled instead.

3 Degenerate Trapezoids

When the line of sight nearly aligns with the light direction—the so-called *dueling frustum* case—the focus area is entirely contained in the far plane, and η may become arbitrarily large, leading to a near-rectangle. This numerically unstable case can be repaired by computing a

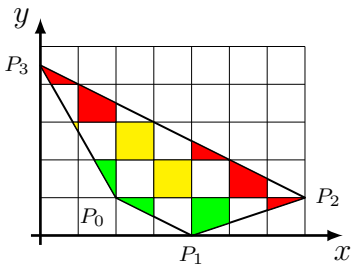

Figure 8: Trapezoid in PPSL.

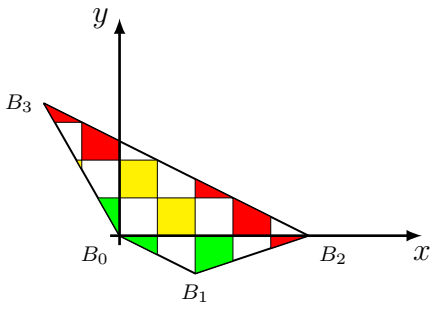

Figure 9: Translate to origin.

true retangular bounding box whenever $\eta > k\lambda$ for some $k \gg 1$. The exact value of k is not critical; 100 to 1,000 work well. For continuity, alignment with the line of sight should be maintained.

The top and base lines computed earlier are valid for the bounding box as well. We need only the left and right edges. This time we project the convex hull vertices onto the left-perpendicular of the unit line of sight vector. This provides the signed distance of each vertex from the line of sight,

$$d_i = \mathbf{a}^{\perp} \cdot (P_i - N) \tag{16}$$

By now our path should be clear. The leftmost and rightmost are given by

$$d_L = \min_i d_i \quad \text{and} \quad d_R = \max_i d_i \tag{17}$$

In this case it is convenient to compute the points where the top and base lines intersect the line of sight,

$$T = N + t_T \mathbf{a} \quad \text{and} \quad B = N + t_B \mathbf{a}\,. \tag{18}$$

Then the bounding box corners are just

$$P_{ij} = i + d_j \mathbf{a}^{\perp}, \tag{19}$$

where again $i \in \{T, B\}$ and $j \in \{L, R\}$.

4 Trapezoidal Projection Matrix

We tried an alternative approach just for fun. The resulting code is slightly more concise than the authors'. Figure 8 dipicts an arbitrary trapezoid in PPSL. We wish to derive the transformation that will take it to x-y clipping coordinates, which for OpenGL consist of the square with diagonal $(-1, -1)$ to $(1, 1)$. Note that in terms of the paper and the previous discussion, edge P_0P_1 is the top line, even though here it appears on the bottom. Similarly P_2P_3 is the bottom line.

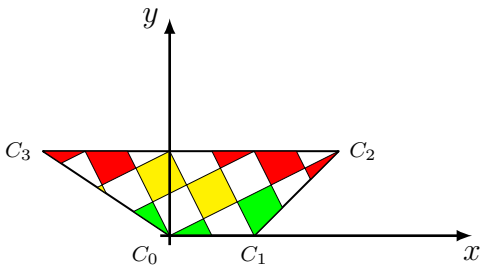

Figure 10: Rotate top edge to x-axis.

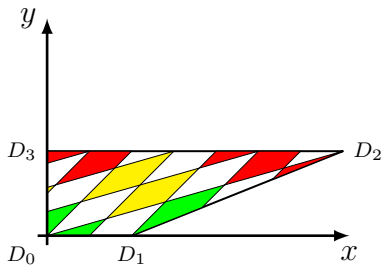

Figure 11: Shear to square one corner.

We begin by translating P_0 to the origin as shown in Figure 9. The required homogeneous transformation matrix is

$$B = \begin{bmatrix} 1 & 0 & -x_{P0} \\ 0 & 1 & -y_{P0} \\ 0 & 0 & 1 \end{bmatrix} . \tag{20}$$

The next step, shown in Figure 10, is to rotate the top line to the x-axis. For this we note that in finding the trapezoid, we have already computed the unit line-of-sight vector $\mathbf{a}$, which provides the needed cosines for the rotation,

$$C = \begin{bmatrix} y_a & -x_a & 0 \\ x_a & y_a & 0 \\ 0 & 0 & 1 \end{bmatrix} . \tag{21}$$

Since we seek an optimized code, pre-multiply by hand to avoid run-time operations:

$$CB = \begin{bmatrix} y_a & -x_a & x_a y_{P0} - y_a x_{P0} \\ x_a & y_a & -(x_a x_{P0} + y_a y_{P0}) \\ 0 & 0 & 1 \end{bmatrix} . \tag{22}$$

Our approach will be to define variables m_{ij} to contain the nontrivial portion of the transformation matrix, updating elements with minimal arithmetic as we proceed with successive concatenations. Thus, the initial code is

$$\begin{aligned} m_{00} &:= y_a & m_{01} &:= -x_a & m_{02} &:= x_a y_{P0} - y_a x_{P0} \\ m_{10} &:= x_a & m_{11} &:= y_a & m_{12} &:= -(x_a x_{P0} + y_a y_{P0}) \; . \end{aligned} \tag{23}$$

The next step is to shear in x to move point C_3 laterally to the x-axis as shown in Figure 11. To find C_3, we use the transform CB already computed by (23) above,

$$\begin{aligned} x_{C3} &:= m_{00} x_{P3} + m_{01} y_{P3} + m_{02} \\ y_{C3} &:= m_{10} x_{P3} + m_{11} y_{P3} + m_{12} \; . \end{aligned} \tag{24}$$

It will be necessary to shear by $-x_{C3}$ in x at $y = y_{C3}$. The desired matrix is

$$D = \begin{bmatrix} 1 & s & 0 \\ 0 & 1 & 0 \\ 0 & 0 & 1 \end{bmatrix} , \text{ where } s = \frac{-x_{C3}}{y_{C3}} . \tag{25}$$

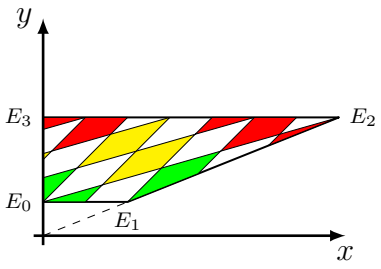

Figure 12: Translate intersection to origin.

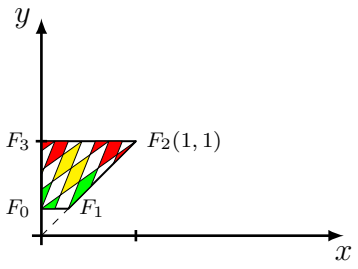

Figure 13: Scale corner to $(1, 1)$.

We now desire the matrix DCB, i.e. the first three operations concatenated. Since we already have CB, we would like to know the necessary update. For this we have

$$D(CB) = \begin{bmatrix} 1 & s & 0 \\ 0 & 1 & 0 \\ 0 & 0 & 1 \end{bmatrix} \begin{bmatrix} m_{00} & m_{01} & m_{02} \\ m_{10} & m_{11} & m_{12} \\ 0 & 0 & 1 \end{bmatrix} = \begin{bmatrix} m_{00} + s\, m_{10} & m_{01} + s\, m_{11} & m_{02} + s\, m_{12} \\ m_{10} & m_{11} & m_{12} \\ 0 & 0 & 1 \end{bmatrix}, \tag{26}$$

which shows that the update is to increment the first row by the second multiplied by s. In code,

$$m_{00} := m_{00} + s\, m_{10} \qquad m_{01} := m_{01} + s\, m_{11} \qquad m_{02} := m_{02} + s\, m_{12}\ . \tag{27}$$

We will repeat this general technique for successive transforms to follow: Inspect the product $Am = m'$ for each new transform A to determine minimal arithmetic that computes m' "in place" by carefully modifying the variables m_{ij}.

As shown in Figure 12, we next move the convergence point of the two non-parallel sides in the positive y-direction to the origin. Point D_2 and the x-coordinate of D_1 provide the displacement. The previous shear operation did not affect y-coordinates. Therefore $y_{D2} = y_{C3}$. The current transformation DCB in Equation 26 provides the remaining unknowns,

$$\begin{aligned} x_{D1} &:= m_{00} x_{P1} + m_{01} y_{P1} + m_{02} \\ x_{D2} &:= m_{00} x_{P2} + m_{01} y_{P2} + m_{02}\ . \end{aligned} \tag{28}$$

The necessary translation matrix is

$$E = \begin{bmatrix} 1 & 0 & 0 \\ 0 & 1 & d \\ 0 & 0 & 1 \end{bmatrix}, \text{ where } d = \frac{x_{D1} y_{D2}}{x_{D2} - x_{D1}}\ . \tag{29}$$

Analysis similar to that in Equation 26 provides the simple update

$$m_{12} := m_{12} + d\ . \tag{30}$$

The next operation must scale E_2 to (1,1) in preparation for the perspective-like transformation that will produce a rectangle. Happily, we can see $x_{E2} = x_{D2}$ and $y_{E2} = y_{D2} + d$.

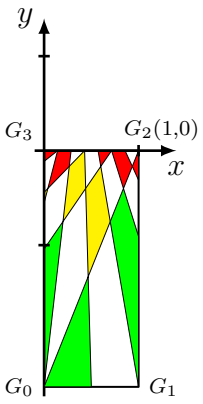

Figure 14: Perspective along y-axis.

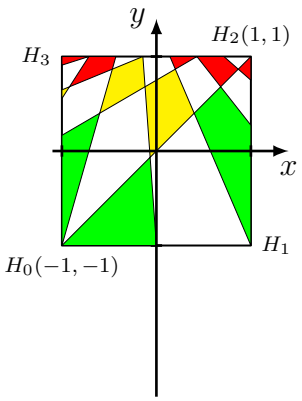

Figure 15: Scale and translate to clip box.

Therefore the desired matrix is the non-uniform scaling

$$F = \begin{bmatrix} s_x & 0 & 0 \\ 0 & s_y & 0 \\ 0 & 0 & 1 \end{bmatrix}, \quad \text{where} \quad s_x = 1/x_{E2} \text{ and } s_y = 1/y_{E2}\ , \tag{31}$$

and the needed update to obtain the next step $FEDCB$ is six multiplications.

$$\begin{aligned} m_{00} &:= s_x\, m_{00} & m_{01} &:= s_x\, m_{01} & m_{02} &:= s_x\, m_{02} \\ m_{10} &:= s_y\, m_{10} & m_{11} &:= s_y\, m_{11} & m_{12} &:= s_y\, m_{12} \end{aligned} \tag{32}$$

The handiest form for the perspective transformation seems to be

$$G = \begin{bmatrix} 1 & 0 & 0 \\ 0 & 1 & -1 \\ 0 & 1 & 0 \end{bmatrix}, \tag{33}$$

with the result shown in Figure 14. This both rectifies the quad and avoids topological mirroring. Pre-multiplying this matrix to form $G(FEDCB)$ copies the second row of the previous matrix to the third, which has until now remained as $[0, 0, 1]$. Then it subtracts one from the last element of the second row. The update is

$$\begin{aligned} m_{20} &:= m_{10} & m_{21} &:= m_{11} & m_{22} &:= m_{12} \\ & & & & m_{12} &:= m_{12} - 1\ . \end{aligned} \tag{34}$$

In the final matrix, we combine scaling followed by translation to gain the desired square in one step. The reader will easily verify that the needed matrix is

$$H = \begin{bmatrix} 2 & 0 & -1 \\ 0 & u & 1 \\ 0 & 0 & 1 \end{bmatrix}, \text{ where } u = \frac{-2}{y_{G0}}\ . \tag{35}$$

The corresponding update is a bit more complicated than previous ones because the last row of the accumulated matrix is no longer a unit-z transformation,

$$\begin{aligned} m_{00} &:= 2\,m_{00} - m_{20} & m_{01} &:= 2\,m_{01} - m_{21} & m_{02} &:= 2\,m_{02} - m_{22} \\ m_{10} &:= u\,m_{10} + m_{20} & m_{11} &:= u\,m_{11} + m_{21} & m_{12} &:= u\,m_{12} + m_{22}\ . \end{aligned} \tag{36}$$

Additional economy is possible by noting that Updates 36 and 32 both scale entire rows. Composing H, G, and F in a single transform on $m = EDCB$ produces

$$HGFm = \begin{bmatrix} 2s_x m_{00} - s_y m_{10} & 2s_x m_{01} - s_y m_{11} & 2s_x m_{02} - s_y m_{12} \\ (u+1)s_y m_{10} & (u+1)s_y m_{11} & (u+1)s_y m_{12} - u \\ s_y m_{10} & s_y m_{11} & s_y m_{12} \end{bmatrix}. \tag{37}$$

Here the third row contains terms that are repeated in the other two. Consequently, careful ordering provides a bit more efficiency than the sequence of Updates 32, 34, 36 that this single one replaces.

$$\begin{aligned} m_{20} &:= m_{10} s_y & m_{21} &:= m_{11} s_y & m_{22} &:= m_{12} s_y \\ m_{10} &:= (u+1) m_{20} & m_{11} &:= (u+1) m_{21} & m_{12} &:= (u+1) m_{22} - u \\ m_{00} &:= (2s_x) m_{00} - m_{20} & m_{01} &:= (2s_x) m_{01} - m_{21} & m_{02} &:= (2s_x) m_{02} - m_{22} \end{aligned} \tag{38}$$

The factors in parentheses should be optimized by the compiler to eliminate redundant computations.

The remaining detail is to compute y_{G0}, which is needed in Equation 35. Observe $y_{E0} = d$, where d was computed in Equation 29. Thus we need only to find the product,

$$FG \begin{bmatrix} 0 \\ d \\ 1 \end{bmatrix} = \begin{bmatrix} 0 \\ s_y\,d - 1 \\ s_y\,d \end{bmatrix}. \tag{39}$$

Perspective division to obtain the true coordinate produces

$$u = \frac{-2}{y_{G0}} = \frac{2 s_y d}{1 - s_y d}\ . \tag{40}$$

5 Degenerate Trapezoids, A Reprise

Again a numerically unstable case occurs when the trapezoid is nearly rectangular. Referring to Equation 29, for such a trapezoid $d \gg 1$, causing translation E to move the quad arbitrarly far from the origin.

The solution is to replace E with a new transform that maps the rectangle with diagonal from the origin to D_2 to our target square. This is certain to cover the frustum even when the bounding quad is slightly tapered.

The value of D_2 is already on hand from Equation 28. The desired matrix is similar to H in Equation 35,

$$E' = \begin{bmatrix} s'_x & 0 & -1 \\ 0 & s'_y & -1 \\ 0 & 0 & 1 \end{bmatrix}, \text{ where } s'_x = \frac{2}{x_{D2}} \text{ and } s'_y = \frac{2}{y_{D2}} . \tag{41}$$

The update is simple, and we must also fill in the third matrix row,

$$\begin{array}{lll} m_{00} := s'_x \, m_{00} & m_{01} := s'_x \, m_{01} & m_{02} := s'_x \, m_{02} - 1 \\ m_{10} := s'_y \, m_{10} & m_{12} := s'_y \, m_{11} & m_{12} := s'_y \, m_{12} - 1 \\ m_{20} := 0 & m_{21} := 0 & m_{22} := 1 \, . \end{array} \tag{42}$$

6 Correcting z

The authors use shader programs to undo distortion in z-coordinates introduced by the trapezoidal transformation. Portability is a difficult and important problem for our application, so we sought to avoid shaders.

We found that by culling front faces during shadow map construction and carefully centering the scene at the origin, we obtained acceptable results with no z-correction. Minor acne on some shadowed faces was the only flaw. Our light source is parallel. This may be an advantage.

An additional problem caused by z-coordinate distortion beyond shadow map offset is its effect on front and back clipping. When we originally positioned the eye point at a virtual light source point far "outside" the scene while rendering the shadow map, z-distortion was so great that front and back clipping removed arbitrary chunks of scene from the shadow map. Since corresonding depth information was missing in the rendering pass, portions of shadows randomly disappeared in the scene. This changed with the trapezoid shape as the viewer's eye moved. It took a day to figure out what was going on! When we set front and back planes far apart to prevent clipping, it was very far indeed. This caused poor shadows due to inadequate depth resolution. The problem was solved by changing the shadow mapping eye point to the center of the scene—possible due to our parallel light source. With this, distortion decreased enough for the algorithm give good results with no z-component correction as mentioned above.

7 Results and Code

In Figure 8 the green-shaded tiles are closest to the frustum eye point. Yellow and red are successively farther away. In Figure 15 the green tiles cover far larger areas, while the red ones have shrunk. This is precisely the intent of the TSM algorithm.

Our implementation is for the West Point Bridge Designer, 2nd Edition. A scene is shown in Figure 16.

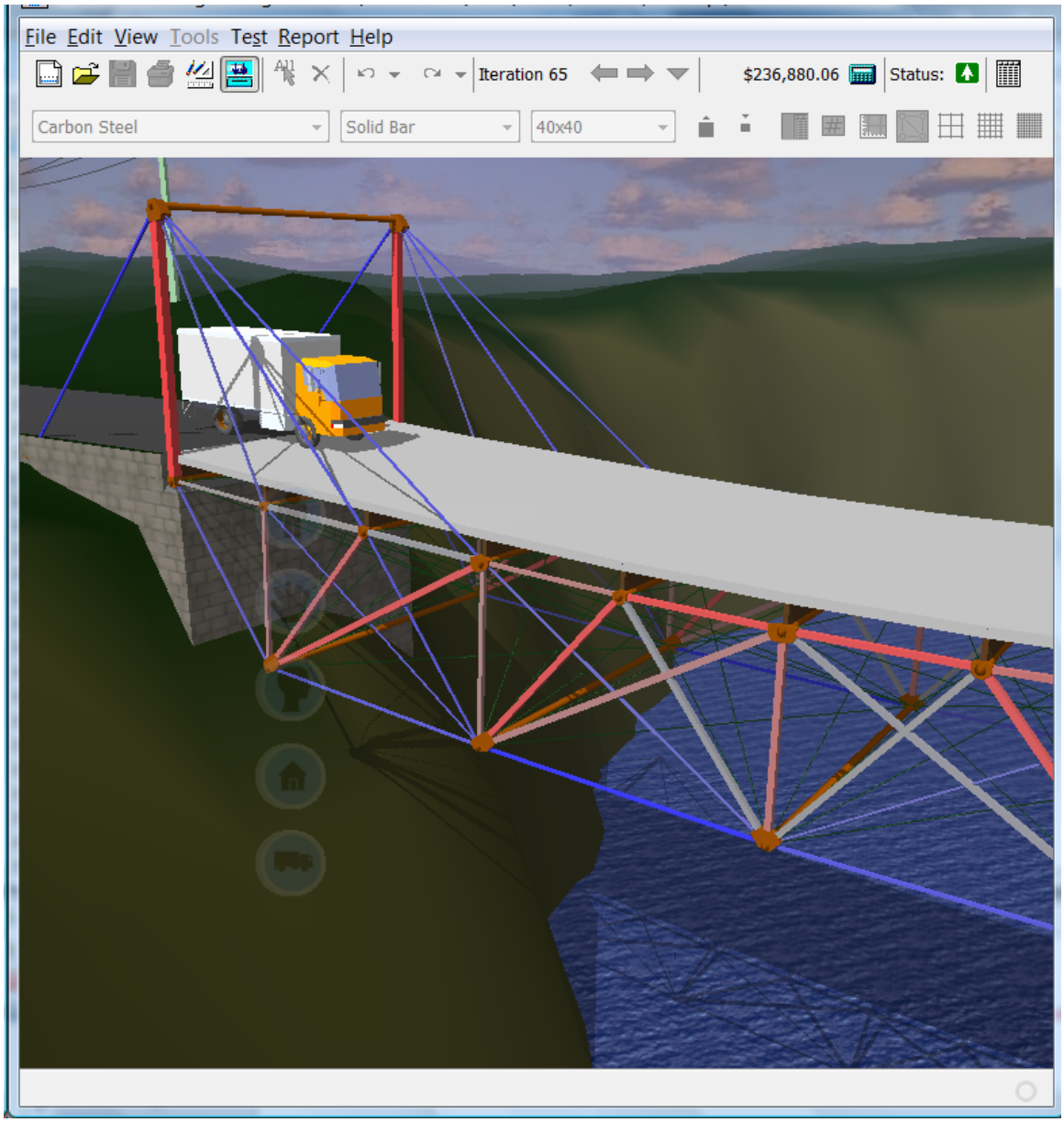

Figure 16: A shadowed scene from the West Point Bridge Designer.

In Figure 17, we implement the logic above in C code, but in a form where the fragment that computes m will transpose easily to many other languages. We have used it in Java, for example.

References

[1] Tiow-Seng Tan Tobias Martin. "Anti-aliasing and Continuity with Trapeziodal Shadow Maps". In: *Proceedings of Eurographics Symposium on Rendering*. Ed. by A.Keller H.W. Jensen. Norrköping, Sweden, June 21–23, 2004, pp. 153–160, 412. URL: `http://www.comp.nus.edu.sg/~tants/tsm/tsm.pdf` (visited on 04/15/2011).

[2] Tiow-Seng Tan Tobias Martin. *Partial source code, Trapezoidal Shadow Maps (TSM)*. Dec. 11, 2004. URL: `http://www.comp.nus.edu.sg/~tants/tsm/tsm_src.zip` (visited on 04/15/2011).

[3] Tiow-Seng Tan Tobias Martin. *Trapezoidal Shadow Maps (TSM)–Recipe*. Feb. 27, 2008. URL: `http://www.comp.nus.edu.sg/~tants/tsm/TSM_recipe.html` (visited on 04/15/2011).

```
#include <stdio.h>
#include <math.h>
void trapezoid_to_clip(double xp0, double yp0, double xp1, double yp1,
                       double xp2, double yp2, double xp3, double yp3) {
  double m00, m01, m02, m10, m11, m12, m20, m21, m22;
  double xa, ya, xc3, yc3, s, xd1, xd2, d, sx, sy, u;

  // Not needed in TSM algorithm: unit LOS vector already computed.
  double dx = xp1 - xp0; double dy = yp1 - yp0;
  double len = sqrt(dx * dx + dy * dy);
  xa = -dy / len; ya = dx / len;

  // ----- Begin fragment to find m. ----------------------------------------
  m00 = ya; m01 = -xa; m02 =   xa * yp0 - ya * xp0;     //                  (23)
  m10 = xa; m11 =  ya; m12 = -(xa * xp0 + ya * yp0);
  xc3 = m00 * xp3 + m01 * yp3 + m02;                    //                  (24)
  yc3 = m10 * xp3 + m11 * yp3 + m12;
  s = -xc3 / yc3;                                       //                  (25)
  m00 += s * m10; m01 += s * m11; m02 += s * m12;       //                  (27)
  xd1 = m00 * xp1 + m01 * yp1 + m02;                    //                  (28)
  xd2 = m00 * xp2 + m01 * yp2 + m02;
  d = yc3 / (xd2 - xd1);                                // yd2 = yc3, start (29)
  if (0 <= d && d < 1e4) {  // Trapezoid case.
    d *= xd1; m12 += d;                                 //           finish (29)
    sx = 2 / xd2; sy = 1 / (yc3 + d);                   //   ye2=yd2=yc3 in (31)
    u = (2 * (sy * d)) / (1 - (sy * d));                //                  (34)
    m20 = m10 * sy;       m21 = m11 * sy;       m22 = m12 * sy; //          (38)
    m10 = (u + 1) * m20;  m11 = (u + 1) * m21;  m12 = (u + 1) * m22 - u;
    m00 = sx * m00 - m20; m01 = sx * m01 - m21; m02 = sx * m02 - m22;
  } else {                  // Near-rectangle case.
    sx = 2 / xd2; sy = 2 / yc3;                         //     yd2 = yc3 in (41)
    m00 *= sx; m01 *= sx; m02 = m02 * sx - 1;
    m10 *= sy; m11 *= sy; m12 = m12 * sy - 1;
    m20 = 0;   m21 = 0;   m22 = 1;
  } // --- Done with fragment to find m. ---------------------------------------
  // Do a trivial test.
#define TRANSFORM_AND_PRINT(P) do {\
    double w = (m20 * x##P + m21 * y##P + m22);\
    double x = (m00 * x##P + m01 * y##P + m02) / w;\
    double y = (m10 * x##P + m11 * y##P + m12) / w;\
    printf(#P " -> (%6.3f, %6.3f)\n", x, y); } while (0)
  TRANSFORM_AND_PRINT(p0); TRANSFORM_AND_PRINT(p1);
  TRANSFORM_AND_PRINT(p2); TRANSFORM_AND_PRINT(p3);
}
int main(void) {
  trapezoid_to_clip(2, 1,   4, 0,   7, 1,  0, 4.5);
  trapezoid_to_clip(1, 1,   3, 2,   2, 4,  0, 3);
  return 0;
}
```

Figure 17: C code with easily portable fragment to compute m.